DOI : https://doi.org/10.7186/wg511202503

Tectono-geomorphic evaluation of Sumatran faults in Bengkulu Segment, Indonesia: Implication to seismic hazard

Anju Goldmoreast Marbun, Edy Sutriyono, Ugi Kurnia Gusti*

Program Studi Teknik Geologi, Universitas Sriwijaya, Jalan Palembang-Prabumulih, KM 32 Inderalaya, Kabupaten Ogan Ilir, Sumatera Selatan 30662, Indonesia

* Corresponding author email address: ugikurnia@unsri.ac.id

Abstrak: Sumatera merupakan salah satu pulau di Indonesia yang dipengaruhi oleh kegiatan tektonik aktif, kerana dikawal oleh interaksi antara lempeng Indo-Australia dan Eurasia. Interaksi antara dua plat litosfera mengakibatkan kemunculan Barisan Orogeny, di mana kawasan lembangan dinaikkan dan sesar aktif dibangunkan di sepanjang pulau. Kajian ini mengkaji peranan Sesar Sumatera dan Sesar Mentawai yang bertanggungjawab terhadap evolusi Lembangan Bengkulu. Penilaian tertumpu pada analisis morfografi Sesar Sumatera (SF) Segmen Bengkulu dan Sesar Alas (AF) dengan pergerakan dip-slip di Renah Gajah Mati I dan sekitarnya di Kabupaten Seluma, Bengkulu. Parameter yang digunakan termasuk "lebar lantai lembah kepada nisbah ketinggian lembah (Vf), pemanjangan lembangan (Re), kamiran hipsometrik (HI), nisbah isipadu kepada kawasan (Rva), dan sinuositi hadapan gunung (Smf)". Hasil analisis menunjukkan AF mempunyai nilai naik yang agak sederhana tinggi berdasarkan nilai plot indeks aktiviti tektonik (IAT) dan ini menunjukkan kawasan tersebut berpotensi terjejas oleh bahaya seismik.

Kata kunci: Tektonik, morfografi, indeks aktivas tektonik, Sesar Alas, Sesar Sumatera

Abstract: Sumatra is one of the islands in Indonesia that is affected by tectonic activitys, because it is controlled by the interaction between the Indo-Australian and Eurasian plates. The interaction between the two lithospheric plates resulted in the emergence of the Barisan Orogeny, where the basin area was uplifted, and active faults were developed along the island. This study examines the role of the Sumatran Fault System (SFS) and the Mentawai Alas Fault System which are responsible for the evolution of the Bengkulu Basin. The evaluation focused on geomorphic analysis of the Bengkulu Segment of the Sumatran Fault (SF) SFS and the Alas Fault (AF) with dip-slip movements in the Renah Gajah Mati and surrounding areas of Seluma Regency, Bengkulu. The parameters used include "valley floor width to valley height ratio (Vf), basin elongation (Re), hypsometric integral (HI), volume to area ratio (Rva), and mountain front sinuosity (Smf)". The results of the analysis show that AF has a relatively medium-high uplift value based on the value of the index of tectonic activity (IAT) plot and this indicates that the area is potentially affected by seismic hazards.

Keywords: Tectonics, morphography, index of tectonic activity, Alas Fault, Sumatran Fault

INTRODUCTION

Sumatra Island, Indonesia, is one of the islands that has high tectonic activity (Ardiansyah, S., 2014), which is located on the southwest edge of Sundaland (Kusnama *et al*., 1992). The Sundaland fragment is an accumulation of continental plates and magmatic arcs originating from Gondwana (Barber & Crow, 2003). Tectonic activity on the island of Sumatra is the subduction of the Indo-Australian Plate with the Eurasian Plate, at a speed of 7 cm/year (Barber *et al*., 2005). In particular, the study area is located in the Bengkulu Basin, the forearc basin, in which it is influenced by two active fault systems, namely the Sumatran Fault System and the Mentawai Alas Fault System (Figure 1) (Mukti *et al*., 2012). One of the products of the tectonic deformation is the presence of the Barisan Orogeny, which crosses Sumatra trending NW-SE (Simandjuntak & Barber, 1996). This orogen is associated with compressional tectonic structures such as folds and thrust belts, and strike slip-faults which play an important role in the formation of relief in the forearc area.

One method for assessing the amount of tectonic activity in the research region is to evaluate the fluvial geomorphic index on the face of the mountain enclosed by faults that exhibit a change in response, including an increase or reduction in the relative tectonic level (Boulton, 2020). The morphometric measurement also

0126-5539; 2682-7549 / Published by the Geological Society of Malaysia.

© 2025 by the Author(s). This is an open access article distributed under the terms of the Creative Commons Attribution (CC-BY) License 4.0

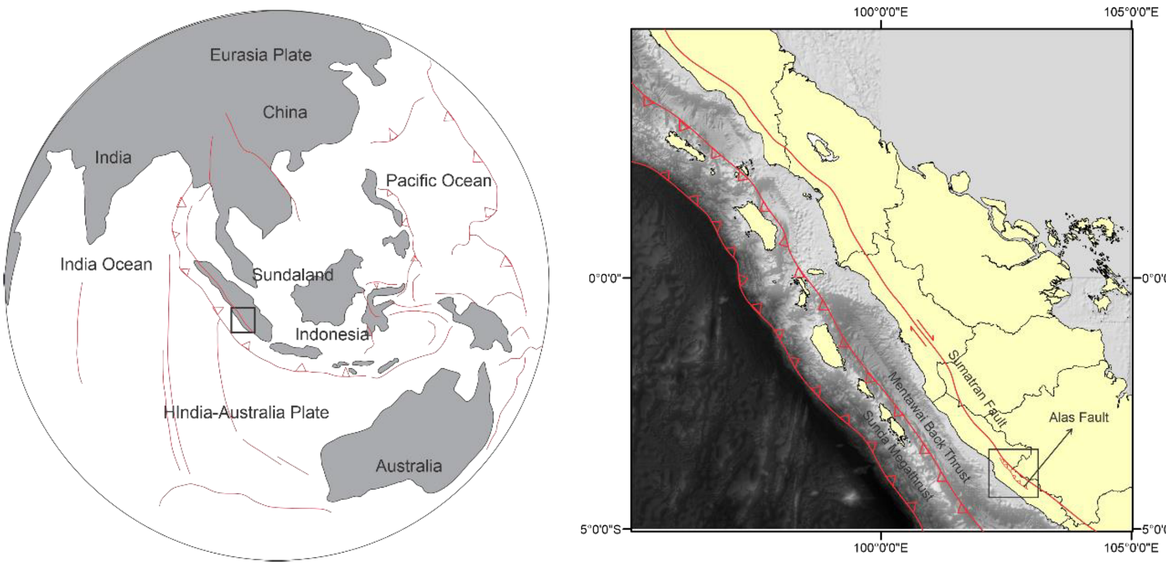

Figure 1: The location of the Alas Fault and the Bengkulu Segment of the Sumatran Fault shown in the black box. Administratively, the research area is in Seluma Regency, Bengkulu, Indonesia. Geographically, the research area is located at coordinates 48 260385 E 9540068 S and 48 269490 E 9521092 S with an area of ± 1,503.03 km^2 (Modified from Daryono *et al*., 2019).

allows for a wider observation area coverage (Snyder *et al*., 2000). Geomorphic indices can be used to measure changes in landforms that have occurred and to analyze the contribution of tectonics in shaping these landforms in various tectonic settings (Chen *et al*., 2003; Yıldırım, 2014; Saber *et al*., 2018; Sahara *et al*., 2022; Gusti *et al*., 2023). It can also determine the relative level of tectonic activity of an area from assessing the topographic response or adjustment to deformation (Keller & Pinter, 2002; Ellis & Barnes, 2015).

Previous studies mainly focused on geological structural properties, kinematics, and neotectonic deformation (Fajri *et al*., 2019; Zuhri & Sutriyono, 2020; Yani & Sutriyono, 2020). The study of relative tectonic activity in the Tanjung Bungo area, West Sumatra (Putri & Hastuti, 2020) explains that the level of tectonic uplift based on geomorphic index analysis in the Tanjung Bungo area, Central Sumatra Basin, has relatively medium-high tectonic activity. The combinations of geomorphic indices have been used successfully in studying the relative tectonic activity of across various geographical areas (e.g. Rockwell *et al*., 1985), such as in Indonesia and around the world.

The results of this study are provided as an estimate of the rate of tectonic uplift along the Alas Fault (AF) and the Bengkulu Segment of the Sumatran Fault (SF) using fluvial geomorphic indices. Another objective of our study is to provide a preliminary evaluation of seismic hazards that have a direct impact on the community. This study employed integrated geomorphic indices based on drainage basins and mountain front ranges to divide the distribution of relative uplift along faults in a ±80 km (AF) and ±50 km (SF) NW-SE orientation (Figure 2). Another objective of our study is to provide a preliminary evaluation of seismic hazards that have a direct impact on the community. This study employed integrated geomorphic indices based on drainage basins and mountain front ranges to divide the distribution of relative uplift along faults in a ±80 km (AF) and ±50 km (SF) NW-SE orientation (Figure 2).

REGIONAL GEOLOGY

The island of Sumatra underwent three distinct stages of tectonic deformation. The first stage involved NW-SE compression during the Late Jurassic – Late Cretaceous period. This was followed by a phase of NS extension during the Late Cretaceous – Early Tertiary. The final stage, occurring from the Middle Miocene to the present, was characterized by NE-SW compression (Pulonggono *et al*., 1992). During this third stage, oblique subduction of the Pacific Oceanic Place under Eurasian Continental Plate occurred, with subduction directions of N 25° E in the southern part of Sumatra Island and N 31° E in the northern part of Sumatra Island, resulting in the formation of a regional strike-slip fault system known as the Sumatran Fault (Hall *et al*., 1993).

The regional geology surrounding the AF has been mapped on a regional scale by Amin *et al*. (1993) and locally in this study near the Renah Gajah Mati 1 Village. The regional geological map (Figure 3) identifies nine geological formations around the AF, and specifically including two formations in the Renah Gajah Mati 1 Village: Hulusimpang Formation, and Seblat Formation.

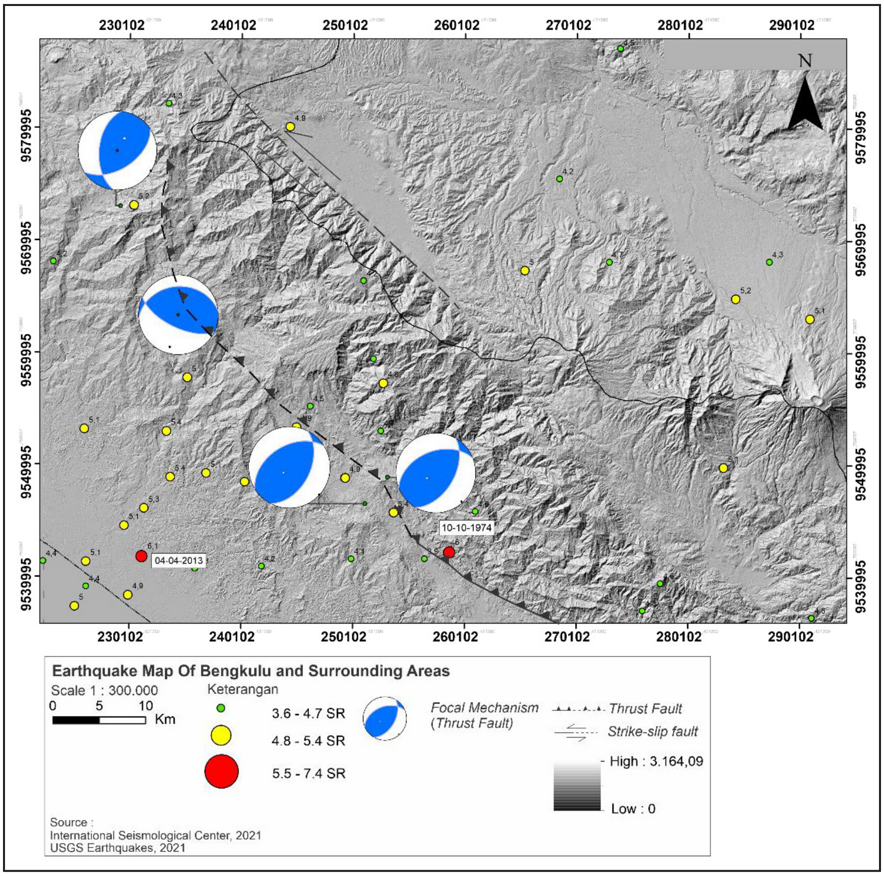

Figure 2: Seismic activity, over the last 50 years, associated with AF and SF in the form of beachball (blue and green balls) (Source: ISC and USGS). Fault withdrawal is based on the results of field observations and data from DEMNas (National Digital Elvation Model).

The Hulusimpang (Oligocene-Early Miocene), which is composed of andesitic-basaltic lava, volcanic breccia, and tuff. This formation covers 15% of the study area in the NE section (Figure 3) and was deposited in a transitional environment during the subsidence phase.

Seblat Formation (Early Miocene – Middle Miocene), deposited in a shallow to deep marine environment. It consists of alternating claystone, calcareous claystone, siltstones, calcareous sandstones, and sandstone nodule. This formation is deposited on top of the Hulusimpang Formation (Yulihanto *et al*., 1995). Subsequently, a granite intrusion (Tmg) intruded through both the Hulusimpang Formation and the Middle Miocene Seblat Formation (Amin *et al*., 1992). Volcanic activity continued to occur through the deposition of the Bal Formation (Tmba), which consists of layered volcanic breccia, tuff, and tuffaceous sandstone nodules (Amin *et al*., 1993).

The Lemau Formation was deposited in the Middle Miocene – Late Miocene (Amin *et al*., 1993) which is conformable with the Seblat Formation. It is composed of claystone, calcareous claystone, coal, sandstone, and conglomerate. This formation is thought to have been deposited in a transitional-shallow marine sea (Yulihanto *et al*., 1995). This formation occupies about 45% of the study area (Figure 3).

The Simpangaur Formation is composed of conglomerate sandstone, sandstone, claystone, with mollusk shells, and sandstone (Amin *et al*., 1993). Deposited in a transitional environment (Yulihanto *et al*., 1995). Then the Bintunan Formation was deposited on top of it, inconsistently, during the Plio - Pleistocene Period. This formation is composed of tuff lithology, polymictic conglomerate, and claystone with lignite insertion. It is covered about 10% of the study area.

MATERIALS AND METHODS

Morphotectonic analysis is a subfield of geomorphology that studies the evolution of continental drift and the influence of tectonic processes (Chebotarev *et al*., 2021). The geometry and appearance of the Earth's surface landforms is known to be the result of specific geological processes (Sunarto, 2004). Morphotectonic calculations, such as those used in this study, are a very useful medium for studying active faults in zones that have active tectonic activity (Cheng *et al*., 2018; Chebotarev *et al*., 2021; Gusti *et al*., 2023). Morphometric measurements of surrounding

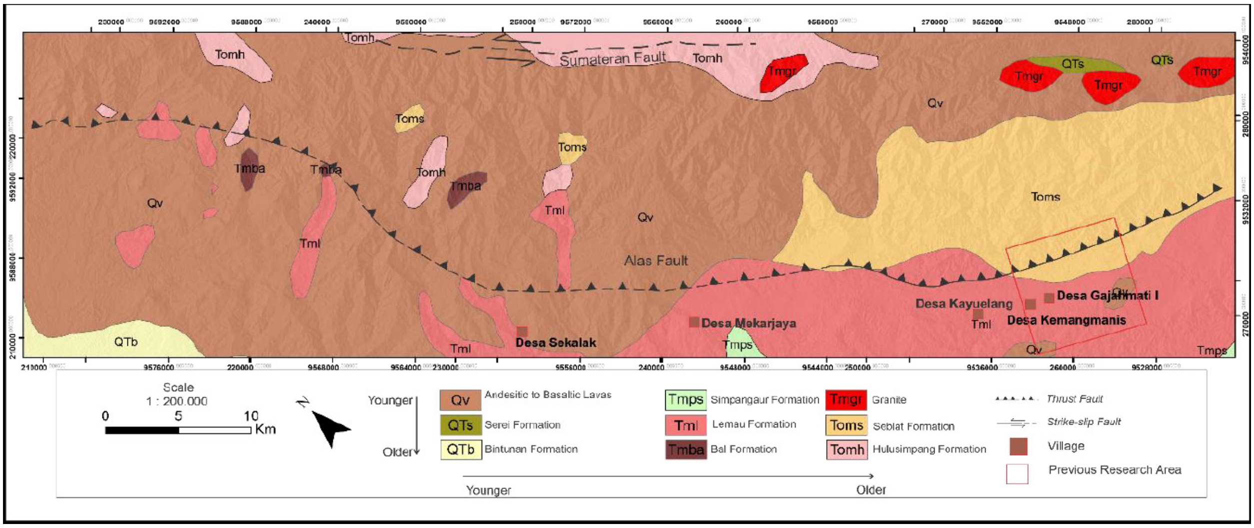

Figure 3: Geological map along the Alas Fault (Modified from Amin *et al*., 1993). Where this fault is caused by the compression regime which resulted in the formation of Orogen Barisan in the Middle Miocene.

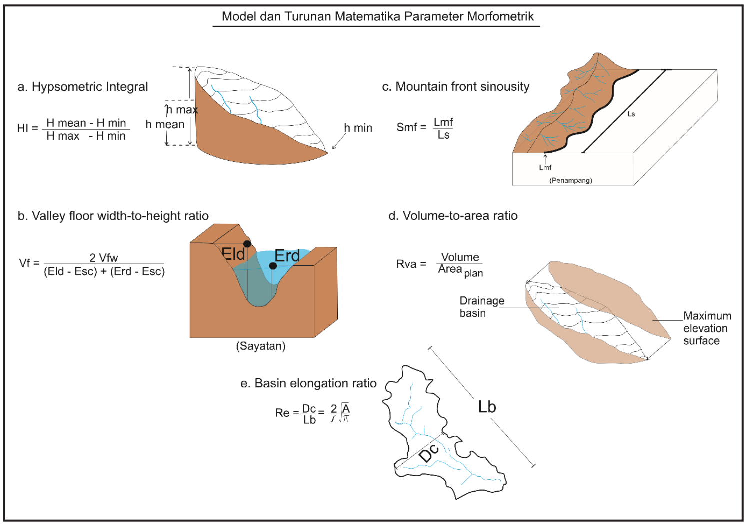

Figure 4: The formula for calculating the morphological index used in the study. (a) hypsometric integral (HI), (b) valley floor width-to-height ratio (Vf), (c) mountain front sinuosity (Smf), (d) volume-to-area ratio (Rva), (e) basin elongation ratio (Re). The results are in the form of numerical data presented in the tabular form.

drainage basins, whose properties are likewise affected by the rate of deformation, were used to assess tectonic activity along the fault (El Hamdouni *et al*., 2008; Cheng *et al*., 2018). The data source in the measurement employs the National Elevation Model Data (DEMNas) with a resolution of 8 meters, as data is collected from Open-sourced DEMNas. DEMNas is the nationwide elevation survey by Indonesia goverment and is the best resolution elevation data in the study area to this current time. The DEM data used to compute morphometric parameters was processed using ArcGIS 10.3.

A drainage basin is an area where the land that receives rainfall is topographically constrained by mountain ridges (Asdak, 2010). Several measurement variables were used in the study of watershed morphometry, including the Hypsometric Integral (HI), Valley floor width-to-height ratio (Vf) (Bull & McFadden, 1977), Volume-to-area ratio (Rva), Basin elongation (Re) (Schumm, 1956), and calculations on mountain front sinousity (Smf) (Figure 4a–e). Based on the distribution of data from each geomorphic index, we classified them into three categories (high, moderate, and low).

Based on the technique presented by El Hamdouni *et al*. (2008), the Index of Tectonic Activity (IAT) may be calculated by dividing the class of each index by the number of extant parameters. The TAI classification includes of five categories, signifying the high tectonic activity along the AF and SF strikes: Class 1 (Very Low), Class 2 (Low), Class 3 (Medium), Class 4 (SHigh), and Class 5 (Very High).

The data for this study was gathered through field observations. The data obtained includes the properties of fault and fold structures. The data collected delivered as geology maps, DEM maps, and Index of Tectonic

Activity (IAT) maps. Geological map presented with a scale of 1:200,000, which is consistent with prior studies; Geological Maps of Manna and Enggano Sheets, and Bengkulu Sheets with a scale of 1:250,000 (Amin *et al*., 1993). Arc GIS 10.3 software was used to generate DEM maps and calculate drainage basin morphometry.

Geomorphic Index

The Geomorphic Index used in this study includes values for the Hypsometric Integral (HI), Mountain Front Sinousity (SMF), Valley Floor width-to-height ratio (Vf), Basin elongation (Re), and volume-to-area ratio (Rva). The data is presented in graphical form as follows:

Hypsometric integral (HI)

The Hypsometric integral (HI) is used to calculate the relative volume of a basin that has not eroded (Strahler, 1952; Schumm, 1956; Cheng *et al*., 2018) (Figure 4a). A high Hypsometric integral value indicates that less material from higher elevations has been eroded, pointing to a relatively young basin produced by considerable uplift (Chen *et al*., 2003). The following equation is used to calculate the value of the hypsometric integral:

$$HI = \frac{H\ mean - H\ min}{H\ max - H\ min}$$

H mean represents the average elevation, *H min* the lowest elevation, and *H max* the maximum height. The geomorphic indices (Figures 5a and 6a) indicate three degrees of tectonic activity: High (HI 0.5), Medium (0.4 HI < 0.5), and Relatively Low (HI < 0.4) (Cheng *et al*., 2018).

Mountain Front Sinousity (Smf)

Mountain Front Sinuosity (Smf) is the ratio of the length of the of the mountain front face along the fault segment to the length of the straight line connecting the points of each segment (Chebotarev *et al*., 2021). The equation to calculate the value of Smf is expressed as follows:

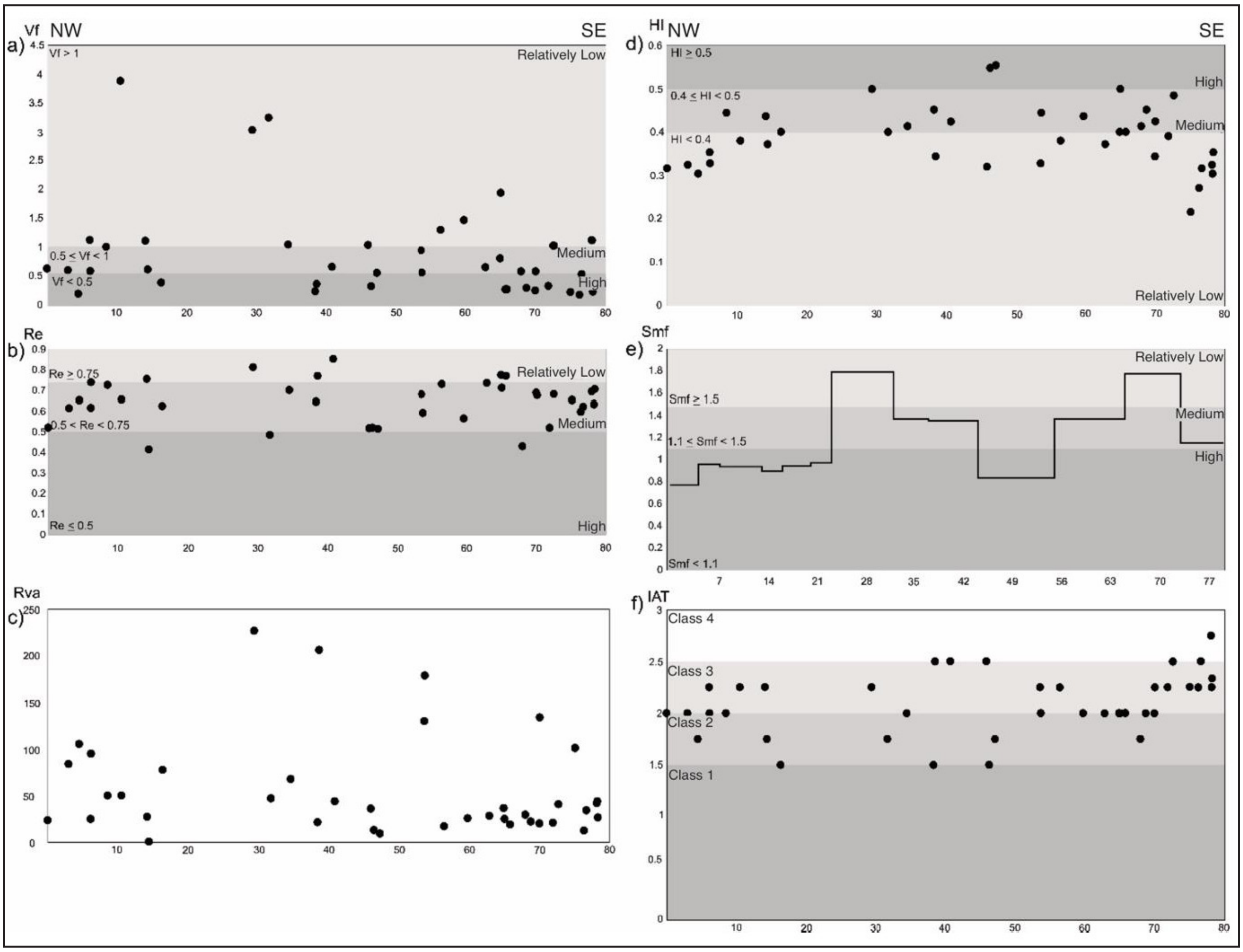

Figure 5: Geomorphic index of the Alas Fault. (a) VF, (b) Re, (c) Rva, (d) HI, (e) Smf, and (f) IAT. The gray gradation depicts the tectonic level based on the assessment of each geomorphic index.

$$Smf = \frac{Lmf}{Ls}$$

Lmf is the total length of the mountain front, measuring a straight line between two end points on the mountain front, while the *Ls* is the sinuous length of the mountain front, measured along its curves. A high Smf value indicates a high level of forefront erosion compared to the uplift process, whereas a low Smf value indicates a level of uplift around the fault segment (Keller & Pinter, 2002; Chebotarev *et al*., 2021). While erosional activity and sediment deposition generate an uneven mountain front, tectonic activity leads to a more linear mountain front. The estimated value of Smf is split into three groups that exhibit lifting activity (Figure 5bb and 6bb): High (Smf < 1.1), Moderate (1.1 Smf < 1.5), and Relatively Low (Smf > 1.5) (El Hamdouni *et al*., 2008).

Basin elongation (Re)

Basin elongation (Re) is the ratio between the diameter and the length of the drainage basin itself (Schumm, 1956). An area with active tectonics is characterized by an elongated basin, on the contrary, an area that with low level of tectonic activity has a drainage basin shape that tends to be circular (Cannon, 1976; Ramírez-Herrera, 1998). The following is an equation for finding the value of Re (Schumm, 1956):

$$Re = \frac{Dc}{Lb} = \frac{2}{l}\frac{\sqrt{A}}{\sqrt{\lambda}}$$

Where *D* is the diameter of the drainage basin; and *L* is the length of the drainage basin. The shape of the basin is identified by the following levels of elongation: circular (0.9-1.0), oval (0.8-0.9), slightly elongated (0.7-0.8), elongated (0.5-0.7), and very elongated (<0.5) (Figueiredo *et al*., 2019; Psomiadis *et al*., 2020). The division of tectonic levels according to Cuong & Zuchiewicz (2001); High (Re 0.5); Medium (0.5 < Re < 0.75); Relatively Low (Re > 0.75) (Figure 5d and 6d).

Volume–to–area ratio (Rva)

The volume-to-area ratio (Rva) describes the ratio between the mean basin depth size, increasing with the rate and number of fault offsets (Schumm & Parker, 1973; Bonnet & Crave, 2003). It is calculated with the following equation:

$$Rva = \frac{Volume}{Area\ plan}$$

Basins with high rate of uplift have Rva values greater than 100, however, not all basins with low Rva values (less than 100) has a low rate of uplift (Frankel & Pazzaglia, 2005). Active uplift of the basin during the construction phase is characterized by a low Rva ratio (Figures 5ee and 6ee).

Index of activate tectonics (IAT)

The Index of activate tectonics (IAT) serves as an assessment or calculation of the level of activity of the Quaternary tectonics (Cheng *et al*., 2018). This calculation identifies tectonic classes (high, moderate, or low) by combining the geomorphic indices (Figure 5 and 6). The result is an indication of the level of tectonic activity (high or active, moderate, and low or inactive) (Saber *et al*., 2018; Saber *et al*., 2020). El Hamdouni *et al*. (2008) validated the value of tectonic classes to quantify the amount of uplift and erosion of rocks from various geomorphic indices using the method:

$$IAT = \frac{S}{n}$$

Where *S* is the sum of each class value and *n* is the number of indexes used. The categories used in this study fall into four IAT classes, ranging from high to very low (Figure 5 and 6) and visualized (Figure 9). Class 1 (1.0 < IAT < 1.5); Class 2 (1.5 < IAT < 2.0); Class 3 (2.0 < IAT < 2.5); and Class 4 (2.5 < IAT < 3.0) (Cheng *et al*., 2018).

RESULTS

In the research area, the AF is approximately 80 km from SE to NW (Figures 2 and 5), whereas the SF is approximately 50 km (Figures 2 and 6a-f). The geomorphic index value along the strike on both faults indicates changes in value that are uniformly distributed in each segment, with a peak at the fault's center. This is demonstrated by different indices with varying values from low to high (Figures 5 and 6). Several geomorphic indices demonstrate minimum rates of uplift at the ends of the faults, with increasing rates towards the middle, as evidenced by lower Smf and Vf values at the NW and SE ends of the faults (Figure 5). It is further corroborated by the low value of Re at the ends of the faults, indicating that the relative uplift rates are low at the ends and increasing towards the middle (Figure 5). The HI geomorphic index similarly indicates that the fault's relative uplift rate is increasing towards the center of the fault, with a high index value and a very low value at the fault's tip while the Rva value displays a low value at both ends (Figure 5).

This study classifies the mean values of each geomorphic index value to reflect the index of tectonic activity (IAT) into four distinct classes (Cheng *et al*., 2018) (Figure 5). The results of the relative uplift rates were consistent across all indices (i.e., moderate to high uplift rates) (Figure 6). It is important to note that the relative uplift rates derived from the geomorphic index may not always be directly proportional to a specific uplift process. This is particularly happening in intraplate areas with low tectonic activity, where other factors like as glacial isostatic adjustment may influence the uplift (Gusti *et al*., 2023). These variations can be attributed to the index's sensitivity to landform maturity, variances in isostatic reaction time, and local variables. The IAT Map (Figure 7) depicts the distribution of the relative tectonic activity index values along the AF in the NW–SE and SE directions, highlighting the relative tectonic activity in each analyzed drainage basin. The study area corresponds to the overall average high relative tectonic activity index value along the SF and AF (Figures 5 and 6).

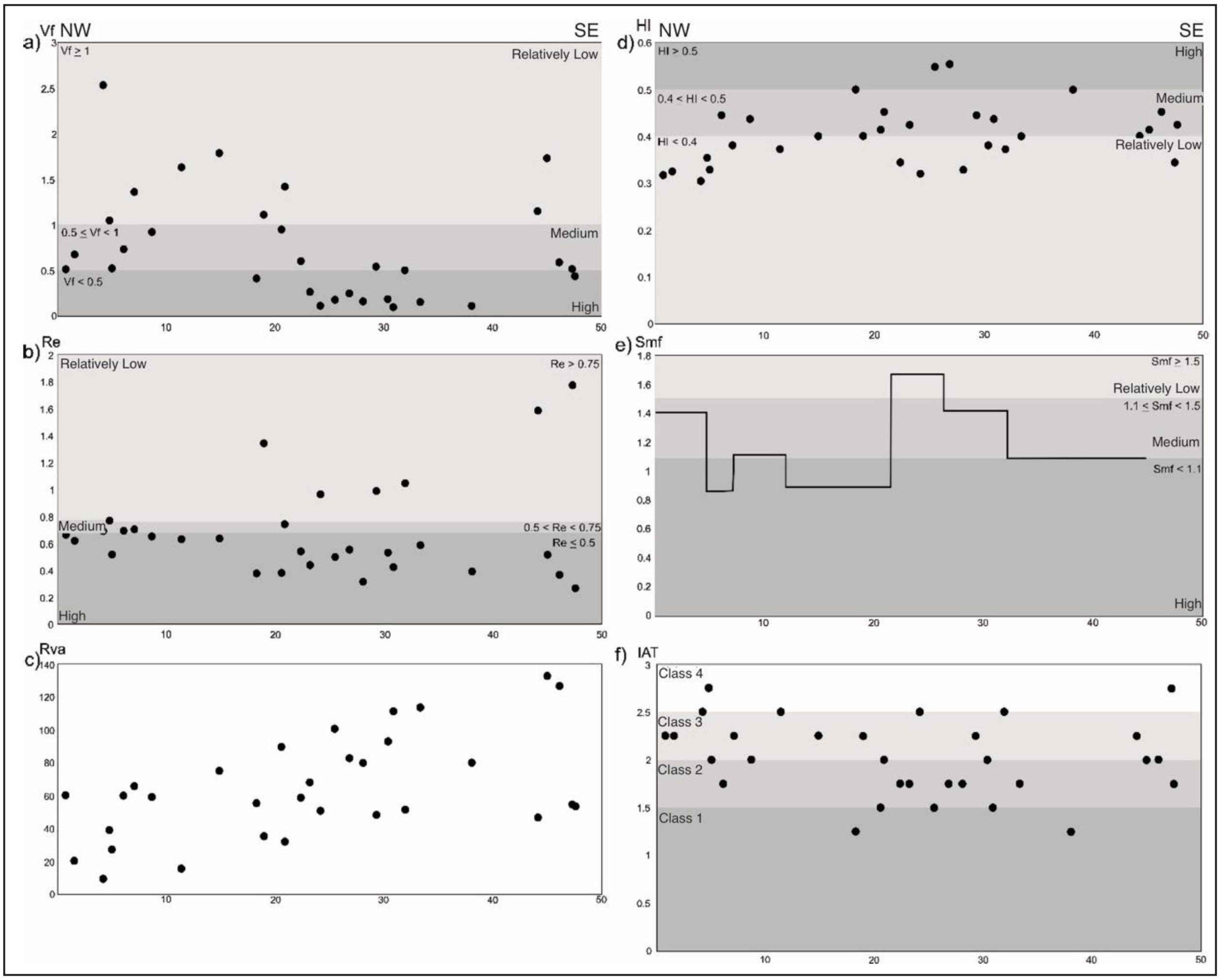

Figure 6: Geomorphic Index of the Sumatran Fault. (a) VF, (b) Re, (c) Rva, (d) HI, (e) Smf, and (f) IAT. The gray gradation depicts the tectonic level based on the assessment of each geomorphic index.

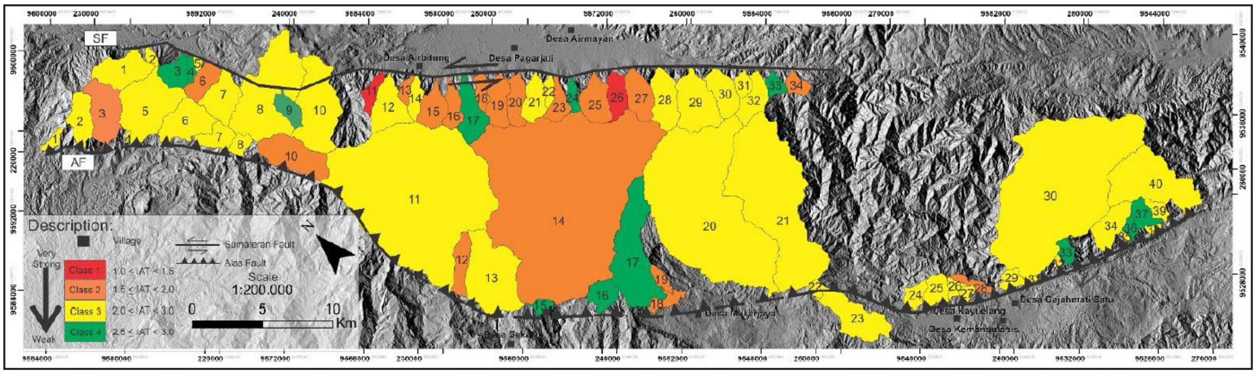

Figure 7: The IAT distribution map based on geomorphic index assessment that occurs along the Alas Fault (bottom) and Sumatran fault (top), Bengkulu. Dominated by yellow and orange colors, which indicate that the research area is affected by moderate – high relative tectonic activity.

DISCUSSIONS

Spatial and temporal uplift patterns along the Bengkulu Segment from the Sumatran fault zone

The integration of several geomorphic indexes and tectonic activity indexes (IAT) in the research area reveals an identifiable distribution pattern extending from the northwest to the southeast. In the study area, the IAT is classified into four classes based on measurements taken in each drainage basin. The distribution of IAT in the studied area shows an interesting pattern, ranging from Northwest to Southeast. In the Northwest, the AF has higher tectonic activity, as evidenced by a high Smf value, suggesting a lower erosion process than morphological uplift, and a high Re value, indicating dominating vertical erosion (Figure 7. AF, drainage basin no. 1- 10). It is comparable to the Southwestern section of the SF, which is dominated by class 3, followed by at least classes 2 and 4, which are associated with low-high relative tectonic activity (Figure. 7. SF, drainage basin no. 1-10).

The SF and AF experienced a high uplift rate across the studied region. This indicates that fault movement from the SF in the Bengkulu Segment and the AF with the highest relative tectonic activity values being in the southern part of Pagarjati Village (Figure 7). This can be seen in the middle of the SF and AF, which border the high morphology, the IAT values are high. Although, the two faults have different kinematic sense of movements, they have the same maximum stress direction from focal mechanism solution of local earthquakes (Figure 2). The activity levels of the two faults increased in the middle, resulting in a high relative uplift rates from the morphology as a result of the interaction of lateral movement of the SF and the uplift of the hanging wall of the AF (Figure 7. AF, drainage basin 11-19) (Figure 7. SF, drainage basins 12-16, 18-23, and 25). In the Southeastern part of AF, the uplift rate is relatively low (Figure 7. AF, drainage basin no. 20-40). Based on this classification, most of the drainage basins show increased tectonic activity from the NW section of the AF and SF (Figures 5-6. f and 7).

Tectonics implication

Several studies have investigated the structural characteristics and kinematics of the AF (e.g., Zuhri & Sutriyono, 2020; Yani & Sutriyono, 2020) and report an average deformation rate of 0.12 - 0.15 mm/year. According to Zuhri & Sutriyono (2020), the structural features observed in the research area are a result of compressional forces during the Late Neogene, resulting in the formation of NW-SE trending faults and folds. Additionally, the Orogen Barisan in the Eastern section of the AF is being uplifted as a result of the ongoing compressional forces (Simandjuntak & Barber, 1996). Moreover, the SF is identified as a dextral strike slip fault that traverses the rear portion of the Orogen Barisan (Sieh & Natawidjaja, 2000).

Our findings corroborated the existence of active Quaternary fault traces cutting through Quaternary deposits, as observed along the Alas Tengah River (Figure 8). Stereographic analysis of the AFS and SFS faults yielded the following results: strike N 275° E, dipping 70° NE, and pitch 50° (Figure 8); strike N 315° E, dipping 82°, and pitch 50° (Figure 8). These two reverse faults exhibit vertical displacement, classifying them as dip-slip dominant faults (Fossen, 2010). The fault traces are linearly connected across drainage basins 27-28, which exhibit moderate to high IAT values (Figure 7). Our findings showed that these two drainage basins have HI, VF, Re, and Smf values that range from moderate to high, and suggesting a relationship with tectonic activity. That results in a convex basin morphology, characterized by dominant vertical erosion and active uplift processes in forearc region of continental arc area. The relatively low Rva value observed is likely indicative of the youth and ongoing development of the drainage basins (Strahler, 1952). Thus, the studied area is experiencing active tectonic deformation and relatively high uplift rates.

Seismic hazards

The study area is located at the forefront of a montain arc and in direct interaction with the subduction between Pacific Plate beneath the Eurasian Plate. This area is highly susceptible to natural hazards, including landslides, volcanic eruptions, earthquakes, tsunamis, and liquefactions.

The findings indicate that specific regions are characterized by elevated tectonic activity, often coinciding with active fault zones. The drainage basin associated with the AF generally exhibits moderate to high IAT values. Furthermore, the area displays significant uplift values, suggesting ongoing tectonic deformation, with multiple geomorphic indices indicating active tectonic deformation. The seismicity linked to subduction along the fault lines, has been recorded over the past 50 years (Figure 2). As a result, this study serves as a foundational reference for identifying potential seismic risks that may have an impact on the local communities. For instance, areas with relatively high uplift rates located near residential area of the local communities, are at an increased seismic risk. Such areas may be more vulnerable to collapse during earthquakes event triggered by rupture along active fault lines. A more detailed assessment of the fault slip rate and geomorphic uplift, quantified over time, would be valuable for zoning areas at risk to earthquakes and ground movement hazards.

CONCLUSIONS

The relative tectonic activity level in the vicinity of the fault zone in the seismically active forearc basin area of Bengkulu has been spatially distributed, as shown by the geomorphic index. The NE and SW portions

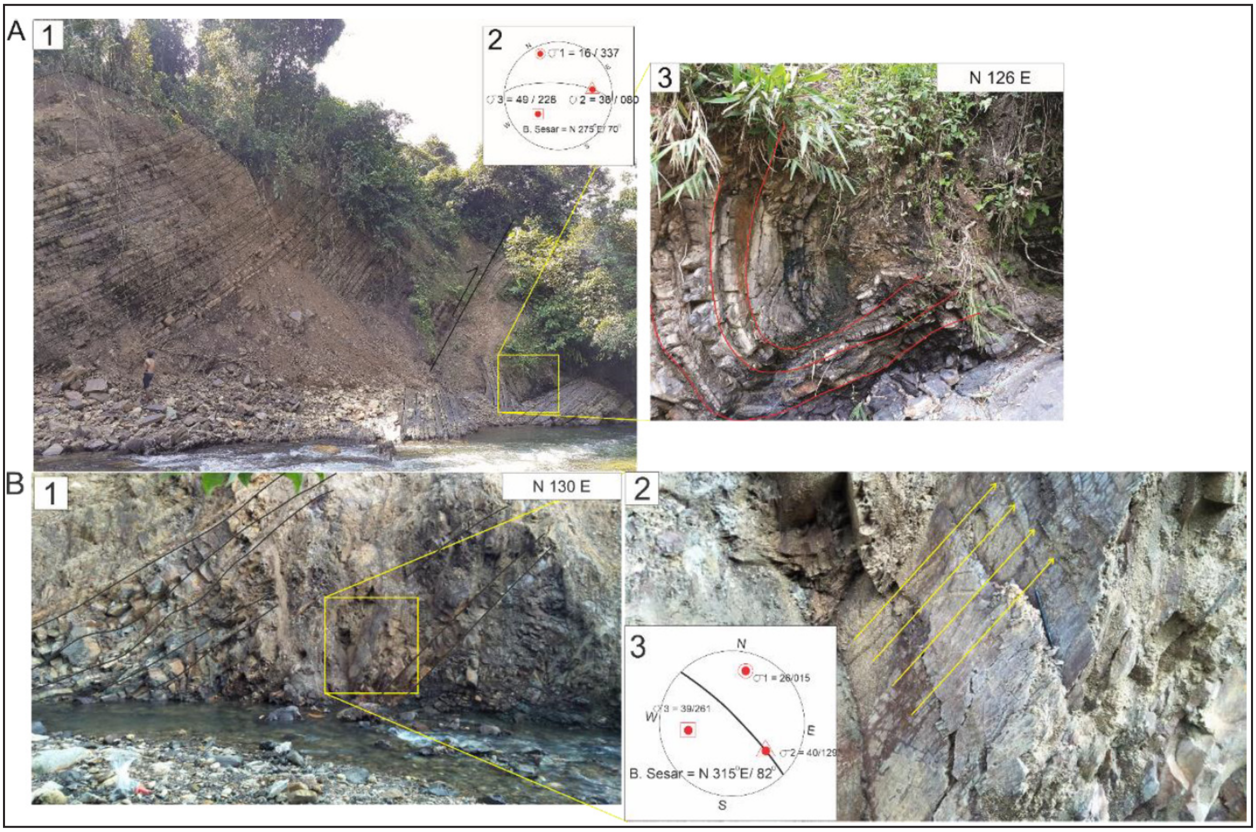

Figure 8: (A) Alas Fault found in Kemang Manis Village and (B) Alas Fault found in Kayu Elang Village, both faults show folding and faulting and have the name dip slip fault (Fossen, 2010). These two evidence of Alas faults are thrust faults that have linear position of drainage basins 27 and 28 which have high IAT value.

that border the Orogen Barisan are home to the AF and the SF. Based on the findings of field observations and morphometric analysis, the research area may be used to reach the following conclusions. The two faults form a general pattern with the direction NW – SE. They were formed as a result of the compression tectonic regime in the Late Neogene which resulted in faults and folds. The AF has a length of approximately 80 km while the SF is 50 km. Kinematically, the AF is a dip slip fault, and the SF is a dextral strike slip fault.

The drainage basin in the study area displays features that are suitable in assessing relative tectonic activity (HI, Smf, Vf, Re, and Rva). In several geomorphic indices, the two faults indicate the rate of tectonic activity from the edge of the fault to the center of the fault. The distribution of the low Vf value in the middle illustrates the number of narrow and steep valleys due to the dominant tectonic activity. The results of Re show that the drainage basin is getting longer in the middle of AF and SF. The Smf values in AF and SF indicate that the front of the mountains mostly describes the process of tectonic activity which is quite dominant compared to the erosional process.

The results of the IAT evaluation show a moderate to high level of tectonic activity (Class 2 to Class 3). For AF, the drainage basin in the Southwest to the Center shows tectonic activity of Class 3 and 2 (moderate – high), while in the Southeastern area of AF shows the levels of Class 4 and Class 3 (low – moderate). Then in SF, the drainage basin of the Southwest to the Center shows tectonic activity from Class 4 to Class 1 (relatively low – relatively high).

ACKNOWLEDGEMENT

Two anonymous reviewers are thanked for their constructive input on this manuscript. We would also like to thank the editorial board of Warta Geologi for handling this manuscript.

AUTHORS CONTRIBUTION

AGM performed interpretation, analysis, drafted and wrote the first manuscript with input from the other authors. AGM conducted field data collection and structural measurements. ES and UKG provided technical oversight, reviewed the writing.

CONFLICT OF INTEREST

This paper has neither been submitted nor published to any journal. There are no competing interests or conflicts of interest associated with this work.

REFERENCES

Amin, T.C., Gafoer, S., & Pardede, R., 1992. Geological Map Sheet Bengkulu, Sumatra. Geological Research and Development Center, Bandung, Scale 1 :250.000, 1 page.

Amin, T.C., Kusnama, Rustandi, E., & Gafoer, S., 1993. Geological Map Sheet Manna & Enggano, Sumatera. Geological Research and Development Center, Bandung, Scale 1 : 250.000, 1 page.

Ardiansyah, S., 2014. Cycle and Estimated Earthquake Occurrence Model in Bengkulu Region. Jurnal Fisika dan Aplikasinya, 10(2), 68-73.

Asdak, C., 2010. Hydrology and Watershed Management: Edisi Revisi V. Gadjah Mada University Press, Yogyakarta. 187 p.

Barber, A.J. & Crow, M.J., 2003. Evaluation of plate tectonic models for the development of Sumatra. Gondwana Research, 20, 1–28.

Barber, A.J., Crow, M.J., & Milsom, J.S., 2005. Sumatera: Geology, Resources and Tectonic Evolution, Geological Society Memoirs No. 31, London.

Bull, W.B., & McFadden, L.D., 1977. Tectonic geomorphology North and South of the Garlock Fault, California. In: Doehring, D.O. (Ed.), Geomorphology in AridRegions: A Proceedings Volume of the 8th Annual Geomorphology Symposium. State University of New York, Binghamton, 115–138.

Bonnet, S., & Crave, A., 2003. Landscape response to climate change: Insights from experimental modeling and implications for tectonic versus climatic uplift of topography. Geology, 31(2), 123-126.

Boulton, S.J., 2020. Geomorphic response to differential uplift: River long profiles and knickpoints from Guadalcanal and Makira (Solomon Islands). Frontiers in Earth Science, 8, 10.

Cannon, P.J., 1976. Generation of Explicit Parameters for a Quantitative Geomorphic Study of The Mill Creek Drainage Basin. Oklahoma Geology Notes, 36, 3–16.

Chebotarev, A., Arzhannikova, A., & Arzhannikov, S., 2021. Long-term Throw Rates and Landscape Response to Tectonic Activity of The Tunka Fault (Baikal Rift) Based on Morphometry, Russia. Tectonophysics, 810, 228864.

Chen, Y.-C., Sung, Q., & Cheng, K.-Y., 2003. Along-strike variations of morphotectonic features in the Western Foothills of Taiwan: tectonic implications based on stream-gradient and hypsometric analysis. Geomorphology, 56(1–2), 109–137. https://doi.org/10.1016/S0169-555X(03)00059-X.

Cheng, Y., He, C., Rao, G., Yan. B., Lin, A., Hu, J., Yu, Y., & Yao, Q., 2018. Geomorphological and structural characterization of the southern Weihe Graben, central China: Implications for fault segmentation, China. Tectonophysics, 722, 11-24.

Cuong, N. Q. & Zuchiewicz, W. A., 2001. Morphotectonic properties of the Lo River Fault near Tam Dao in North Vietnam. Nat. Hazards Earth Syst. Sci., 1, 15–22. https://doi.org/10.5194/nhess-1-15-2001, 2001.

Daryono, M.R., Natawidjaja, D.H., Sapiie, B., & Cummins, P., 2019. Earthquake Geology of Lembang Fault, West Java, Indonesia. Tectonophysics, 751, 180-191.

El Hamdouni, R., Irigary, C., Fernández, T., Chacón, J., & Keller, E.A., 2008. Assesment of Relative Active Tectonics, Southwest Border of Sierra Nevada (Southern Spain). Geomorphology, 96, 150-173.

Ellis, M.A., & Barnes, J.B., 2015. A global perspective on the topographic response to fault growth. Geosphere, 11(4), 1008–1023.

Fajri, S.N., Sutriyono, E., & Nalendra, S., 2019. Lineament analysis of digital elevation model to identification of geological structure in Northern Manna Sub-Basin, Bengkulu. International Conference on Architecture and Civil Engineering (ICACE), OP Conf. Ser.: Mater. Sci. Eng., 636 012001.

Figueiredo, P.M., Rockwell, T.K., Cabral, J., & Ponte Lira, C., 2019. Morphotectonics in a low tectonic rate area: Analysis of the southern Portuguese Atlantic coastal region. Geomorphology, 326, 132–151. https://doi.org/10.1016/j.geomorph.2018.02.019.

Fossen, H., 2010. Structural Geology. Cambridge University Press, New York. 463 p.

Frankel, K.L., & Pazzaglia, F.J., 2005. Tectonic Geomorphology, Drainage Basin Metrics, and Active Mountain Fronts. Geografia Fisica e Dinamica Quaternaria, 28(1), 7–21.

Gusti, U.K., Peace, A.L., & Rimando, J., 2023. Tectonic geomorphology of the Ottawa-Bonnechere Graben, Eastern Canada: implications for regional uplift and intraplate seismicity. Canadian Journal of Earth Sciences, 60, 635–652. https://doi.org/10.1139/CJES-2022-0137.

Hall, D.M., Buff, B.A., Courbe, M.C., Seurbert, B.W., Siahaan, M., & Wirabudi, A.D., 1993. The Southern Fore-Arc Zone of Sumatera: Cainozoinc Basin-Forming Tectonism and Hidrocarbon Potensial. Proceedings 22nd Annual Convention, IPA, 319-334.

Keller & Pinter, 2002. Active Tectonics: earthquakes, uplift, and landscape. Prentice Hall, Upper Saddle River, NJ. 362 p.

Kusnama, Mangga S.A. & Sukarna, D., 1992. Tertiary Stratigraphy and Tectonic Evolution of Southern Sumatra. Geological Society of Malaysia-Circum-Pacific For Energy And Mineral Resources Tectonic Framework And Energy Resource of The Western Margin of Pacific Basin, Kuala Lumpur, 143-152.

Mukti, M.M., Singh, S.C., Deighton, I., Hananto, N.D., Moeremans, R., & Permana, H., 2012. Structural evolution of backthrusting in the Mentawai Fault Zone, Offshore Sumatran Forearc. Geochemistry, Geophys. Geosystems, 13, 1–21.

Psomiadis, E., Charizopoulos, N., Soulis, K.X., & Efthimiou, N., 2020. Investigating the correlation of tectonic and morphometric characteristics with the hydrological response in a Greek river catchment using earth observation and geospatial analysis techniques. Geosci., 10, 1–30. https://doi.org/10.3390/geosciences10090377.

Pulonggono, A., Haryo, S.A., & Kosuma, C.G. 1992. Pre-Tertiary Fault System as a Framework of The South Sumatera Basin; a Study of Sar-maps. Proceedings 21st Annual Convention, IPA, 339-360.

Putri, D.A., & Hastuti, E.W., 2020. Morphotectonic analysis of Tanjung Bungo area based on geological structure control, Central Sumatera Basin. Proceedings Indonesian Petroleum Association, IPA20-SG-254.

Ramírez-Herrera, M.T. 1998. Geomorphic assessment of active tectonics in the Acambay Graben, Mexican volcanic belt. Earth Surface Processes and Landforms, 23, 317–332.

Rockwell, T.K., Keller, E.A., & Jhonson, D.L., 1985. Tectonic geomorphology of alluvial fans and mountain fronts near Ventura, California. In: Morisawa, M. (Ed.), Tectonic Geomorphology. Proceedings of the 15th Annual Geomorphology Symposium. Allen and Unwin Publishers, Boston, 183 – 207.

Saber, R., Caglayan, A., & Isik, V., 2018. Relative tectonic activity assessment and kinematic analysis of the North Bozgush fault Zone, NW Iran. J. Asian Earth Sci., 164, 219–236. https://doi.org/10.1016/J.JSEAES.2018.06.023.

Saber, R., Isik, V., & Caglayan, A., 2020. Tectonic geomorphology of the Aras drainage basin (NW Iran): Implications for the recent activity of the Aras fault zone. Geol. J., 55, 5022–5048. https://doi.org/10.1002/GJ.3724.

Sahara, R., Fadhli, M., & Gusti, U.K., 2022. Morphotectonic Analysis of South Solok Area: Implication for Geothermal Manifestation and Relative Tectonic Activity. Journal of Geology Sriwijaya, 1, 37–46. https://doi.org/10.5281/ZENODO.8240473.

Schumm, S.A., 1956. Evolution of drainage systems and slopes in badlands at PerthAmboy, New Jersey. Geol. Soc. Am. Bull., 67(5), 597–646.

Schumm, S.A. & Parker, R.S., 1973. Implications of complex response of drainage systems for Quaternary alluvial stratigraphy. Nature, Phys. Sci., 243, 99-100.

Sieh, K. & Natawidjaja, D., 2000. Neotectonics of the Sumatran fault, Indonesia. Journal of Geophysical Research: Solid Earth, 105(B12), 28295-28326.

Snyder, N.P., Whipple, K.X., Tucker, G.E., & Merritts, D.J., 2000. Landscape response to tectonic forcing: Digital elevation model analysis of stream profiles in the Mendocino triple junction region, northern California. Geol. Soc. Am. Bull., 112, 1250–1263. https://doi.org/10.1130/0016-7606(2000)112<1250:LRTTFD>2.0.CO;2.

Simandjuntak, T.O. & Barber, A.J., 1996. Contrasting tectonic styles in the Neogen orogenic belts of Indonesia. In: Hall, R. & Blundell, D., (Eds.), Tectonic Evolution of Southeast Asia. Geological Society Sprecial Publication, 106, 185-201.

Strahler, A.N., 1952. Hypsometric (area-altitude) analysis of erosional topography. Geological Society of America Bulletin, 63(11), 1117-1142.

Sunarto, S., 2004. Geomorphic changes in coastal area surround Muria Volcano. Doctoral dissertation, Gadjah Mada University Yogyakarta, Indonesia.

Yani, S., & Sutriyono, E., 2020. The structural pattern of the Kemang Manis area and its surroundings, Seluma Regency, Bengkulu. Journal of Earth and Energy, 1, 43-49.

Yıldırım, C., 2014. Relative tectonic activity assessment of the Tuz Gölü Fault Zone; Central Anatolia, Turkey. Tectonophysics, 630, 183–192. https://doi.org/10.1016/j.tecto.2014.05.023.

Yulihanto, B., Situmorang, B., Nunjajadi, A., & Sain, B., 1995. Structural Analysis of The Onshore Bengkulu Forearc Basin and its Implication for Future Hydrocarbon Exploration Activity. Proceedings Indonesian Petroleum Association, 24th Annual Convention, 85-96.

Zuhri, W., & Sutriyono, E., 2020. Late Neogen Deformation of Rock Succession at Renah Gajah Mati I Region Seluma Regency in Bengkulu. Jurnal Teknologi, 82(2), 77-83.

Manuscript received 19 March 2024;
Received in revised form 20 June 2024;
Accepted 31 January 2025
Available online 30 April 2025